sustainability

MDPI

Article

An Explicit Model for Optimal Siting and Sizing of Electric Truck Charging Stations

Yang Xu [1], Xia Shang [1], Yeying Wang [2] and Lihui Zhang [1,*]

[1] Institute of Intelligent Transportation Systems, Zhejiang University, Hangzhou 310058, China; xxuyang99@zju.edu.cn (Y.X.); shangxia@zju.edu.cn (X.S.)
[2] Polytechnic Institute, Zhejiang University, Hangzhou 310015, China; 22360193@zju.edu.cn
* Correspondence: lihuizhang@zju.edu.cn; Tel.: +86-185-0581-1559

Abstract

The deployment of electric trucks is recognized as a crucial tool for reducing dependence on traditional fossil fuels and mitigating pollution from transportation systems. However, insufficient and unbalanced distribution of charging stations may hinder the use of electric trucks. This study develops an explicit mixed-integer linear program to optimize the siting and sizing of charging stations for electric trucks in general transport networks. The model incorporates the queuing dynamics of electric trucks at charging stations through a formulated set of first-come-first-served constraints, enabling the direct computation of the charging waiting time for each truck. The objective function minimizes the total system cost, comprising the charging station construction cost, the electric truck procurement cost, the electricity consumption cost, and the operational cost, consisting of travel times, queuing times, and the delay penalties of the trucks. To address the computational challenges in solving large-scale network problems, we propose a hybrid solution strategy combining a rolling horizon framework with a genetic algorithm, which enhances computational efficiency through problem decomposition and iterative optimization. Finally, numerical experiments are conducted on three road networks, including the Sioux Falls network and the Chicago network, to validate the effectiveness of the proposed model and algorithm.

Keywords: highway transportation; electric truck; charging station; charging queue; siting and sizing; vehicle routing

check for updates

Academic Editor: Antonio P. Gutierrez de Blume

Received: 20 October 2025
Revised: 14 November 2025
Accepted: 26 November 2025
Published: 29 November 2025

Citation: Xu, Y.; Shang, X.; Wang, Y.; Zhang, L. An Explicit Model for Optimal Siting and Sizing of Electric Truck Charging Stations. *Sustainability* **2025**, *17*, 10708. https://doi.org/10.3390/su172310708

Copyright: © 2025 by the authors. Licensee MDPI, Basel, Switzerland. This article is an open access article distributed under the terms and conditions of the Creative Commons Attribution (CC BY) license (https://creativecommons.org/licenses/by/4.0/).

1. Introduction

As the transport system is a key sector for energy consumption and greenhouse gas emissions, its green transition plays an important role in achieving carbon neutrality for the world. Fostering and developing clean energy vehicles is regarded as one crucial pathway. This study focuses on electric freight trucks.

The large-scale adoption of electric freight trucks requires the scientifically grounded layout of charging infrastructures. Recent studies have emphasized that balancing vehicle deployment with infrastructure rollout has become a critical policy and research priority for enabling low-carbon trucking [1–4]. This coordination challenge is particularly acute for freight transportation, where the economic viability of electric truck adoption hinges on the synchronized development of vehicles and charging infrastructure. Our modeling framework tries to jointly optimize the siting and sizing of charging stations, as well as the fleet size and routing plans of electric trucks, thereby contributing to the development of coordinated transition strategies for sustainable freight transportation.

In the literature, extensive research has been conducted on the siting and sizing of charging stations for various types of electric vehicles. For example, Song [5] proposed a model to optimize the spatial layout of charging stations based on the analysis of the quantitative relationship between the charging facility supply and the charging time cost. Zhu et al. [6] formulated a mixed-integer linear program (MILP) to jointly optimize the siting and sizing of charging stations, aiming to minimize the infrastructure construction cost and vehicle travel cost. Seifeddine et al. [7] proposed an MILP model based on a weighted set-covering concept. By introducing a concept of coverage radius, the model incorporates users' acceptable travel distance as a critical behavioral factor in the decision process. Shang et al. [8] developed an integrated planning model for public charging stations and private charging piles under a steady-state charging demand assumption to quantify the optimal settings of the two types of facilities. Xiao et al. [9] constructed a bi-level programming model in which the upper level balances annual station costs and user costs to make siting decisions, while the lower level partitions service areas based on a shortest path principle. Then, a simulated annealing–Dijkstra hybrid algorithm was designed to solve the model efficiently.

The configurations of the charging network will directly influence the route choices of electric vehicles and thereby the overall freight efficiency. Thus, a growing body of work integrates the vehicle routing problem into the framework of the siting and sizing of charging facilities. For instance, Zhu et al. [10] introduced a behavioral parameter named path deviation tolerance and, by modeling drivers' willingness to detour from their normal routes, examined how route choice preferences influence the siting decisions for charging stations. Sun et al. [11] developed a joint optimization model that couples electric truck routing with charging facility layout in bidirectional transport scenarios, and applied a hybrid metaheuristic combining genetic algorithms with tabu search to solve it. Wang et al. [12] proposed a multi-objective model for multi-depot–multi-period scenarios to generate Pareto frontiers for charging station locations and vehicle travel routes. Wu et al. [13] investigated a multi-stage charging station deployment problem that considers the construction cost, travel time cost, and carbon emission cost. An improved particle swarm algorithm was applied to optimize the coupled transport and power systems. Kınay et al. [14] formulated a bi-level program for siting and sizing of charging facilities, considering stochastic traffic flows and uncertain charging times. The upper level determines the station locations and capacities, while the lower level captures user route choice behaviors. In parallel, significant advances have been made in stochastic routing methodologies that address operational uncertainties. For example, Yi and Bauer [15] proposed a stochastic programming problem to find the minimum energy routes for electric vehicles, considering the random effects of environmental factors on transport energy cost. Owais and Alshehri [16] delivered a vehicle routing technique for transportation networks under demand uncertainties to find a set of Pareto optimal shortest paths. Almutairi and Owais [17] introduced a reliable vehicle routing framework using traffic sensor-augmented information, and demonstrated how real-time data could enhance routing reliability under uncertain conditions.

However, most of the existing studies considering vehicle routing do not fully account for the impact of charging dynamics at charging stations. With heavy traffic and high charging demand, unbalanced station layouts may lead to excessive overload of certain charging stations and trigger substantial queuing delays there. To deal with this issue, some studies have tried to model the queuing dynamics at charging stations. Setak et al. [18] constructed a vehicle routing model with charging queues based on multigraph theory, and the waiting times at charging stations were derived based on M/M/s queuing systems. Li et al. [19] developed an MILP for routing electric vehicles, in which waiting times at charging stations were estimated with a bespoke heuristic algorithm. Chen et al. [20]

incorporated queuing delays and user route choices into their siting and sizing model for charging stations. Charging queues were first simulated using M/M/s queuing systems, after which waiting time distributions were estimated via the least squares method. Uslu et al. [21] also considered queuing times in their siting and sizing model. The levels of service at charging stations were enforced via capacity constraints, and the queuing times of charging vehicles were estimated with M/M/1 queuing systems. Schoenberg et al. [22] utilized historical charging data to estimate waiting times for future time periods, so as to better facilitate decision-making for building charging stations.

The above studies have tried to consider waiting times at charging stations, and most of them rely on queuing theory. However, such approaches typically formulate optimization problems into mathematical programs with implicit constraints, which are difficult to solve directly using standard optimization algorithms. This feature may limit the further development of these proposed models. To this end, this paper develops an explicit MILP model for the siting and sizing of charging facilities for electric freight trucks. Rather than relying on queuing theory, we construct a set of mathematical constraints that enforce the first-come-first-served principle at charging stations, and enable direct computation of the charging waiting time for each truck. For small-scale problems, commercial solvers can be directly applied to generate the optimal solutions. For large-scale problems, a hybrid solution strategy that combines the rolling horizon framework with a genetic algorithm is further proposed.

2. Problem Statement

As illustrated in Figure 1, the area deploys an electrified logistic system for freight delivery between internal origin–destination (OD) pairs. Each electric truck departs from its original start point, and travels to a customer node with a start depot to pick up customer goods and then deliver them to the corresponding drop-off node with an end depot. This process continues iteratively according to subsequent delivery tasks. The state of charge (SoC) of each electric truck is monitored in real time. If the SoC is insufficient, the truck first detours to a charging station to recharge to full power (which can be relaxed to like 90%) before resuming service. The charging network will first be built to satisfy the charging demand of electric trucks in service. It is assumed that all the dynamic system information regarding the delivery tasks, the electric trucks, the charging infrastructures, and the road network, is fully known to a central decision-maker. The decision-maker optimizes the routing and charging plans for all the trucks in advance according to the delivery tasks, while truck drivers only need to execute the prescribed plans without making any operational decisions, except for in emergencies.

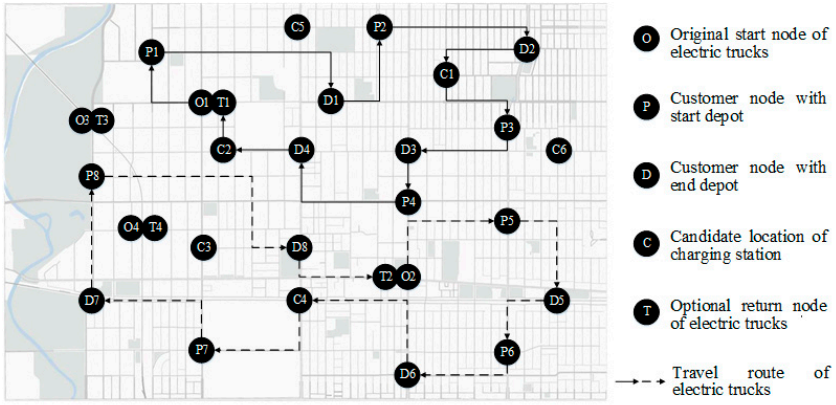

Figure 1. Serving routes of electric trucks.

This study develops an explicit mathematical program to optimize the above electrified logistic system so that both the logistic demand and the vehicle charging demand can be well served. The model jointly optimizes the locations of charging stations, the capacity of each charging station, the fleet size of electric trucks and the routing plans of all the trucks. The objective is to minimize the total system cost comprising the charging station construction cost, the electric truck procurement cost, the electricity consumption cost, and the operational cost composed of travel times, queuing times, and the delay penalties of the trucks.

Specifically, the model to be delivered explicitly captures the queuing dynamics of electric trucks at all the charging stations. As shown in Figure 2, electric trucks will be served following the first-come-first-served principle, i.e., a truck arrived earlier is required to be served before any other truck that arrives later. While overtaking, preemption or priority insertion is not permitted. There is only one queue, if any, at each charging station. Upon arrival, each truck must join the queue, if any, before it can be served.

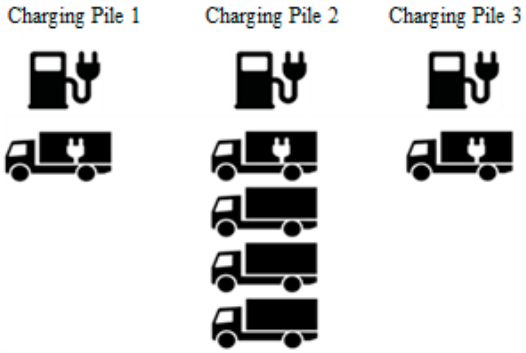

Figure 2. Queuing of electric trucks at charging stations.

3. Model Formulation

The notations used in the model are summarized in Table 1. The detailed mathematical formulation is presented below.

Table 1. Notations.

Symbol		Description
Sets	O	Set of original start points of electric trucks. There are in total σ optional start points, so $O = \{1, 2, \ldots, \sigma\}$
	P	Set of customer nodes with start depots. There are δ delivery demands, so $P = \{\sigma + 1, \sigma + 2, \ldots, \sigma + \delta\}$
	D	Set of customer nodes with end depots. Each delivery task corresponds to a node pair of origin and destination, so $D = \{\sigma + \delta + 1, \sigma + \delta + 2, \ldots, \sigma + 2\delta\}$
	C_n	Set of candidate charging pile nodes at station n. The allowed maximum number of charging piles at station n is $R_{n,\max}$, so $C_n = \{\sigma + 2\delta + R_{1,\max} + R_{2,\max} + \ldots + R_{n-1,\max} + 1, \sigma + 2\delta + R_{1,\max} + R_{2,\max} + \ldots + R_{n-1,\max} + 2, \ldots, \sigma + 2\delta + R_{1,\max} + R_{2,\max} + \ldots + R_{n-1,\max} + R_{n,\max}\}$
	C	Set of all candidate charging pile nodes across all stations. The allowed maximum number of charging piles is $Q_{\max}$, so $C = C_1 \cup C_2 \cup \ldots \cup C_n = \{\sigma + 2\delta + 1, \sigma + 2\delta + 2, \ldots, \sigma + 2\delta + Q_{\max}\}$
	T	Set of optional return points of electric trucks, which can be the same as their original start points, so $T = \{\sigma + 2\delta + Q_{\max} + 1, \sigma + 2\delta + Q_{\max} + 2, \ldots, 2\sigma + 2\delta + Q_{\max}\}$
	N	Set of all nodes, $N = O \cup P \cup D \cup C \cup T$
	U	Set of candidate locations for charging stations. There are $n_{\max}$ candidate charging stations, so $U = \{1, 2, \ldots, n_{\max}\}$
	V	Set of all available electric trucks. Let the allowed maximum number of electric trucks be $V_{\max}$, then $V = \{1, 2, \ldots, V_{\max}\}$

Table 1. *Cont.*

Symbol		Description
Parameters	d_{ij}	The shortest distance between node $i \in N$ and node $j \in N$
	t_{ij}	Travel time from node $i \in N$ to node $j \in N$, which is equal to d_{ij} divided by the average driving speed
	a_i	The start time of the delivery task at customer node $i \in P$
	c_t	Unit travel time cost of electric trucks
	c_e	Unit electricity consumption cost
	c_f	Procurement and maintenance cost of each electric truck
	c_s	Construction and maintenance cost of each charging station
	c_r	Construction and maintenance cost of each charging pile
	c_q	Unit waiting time cost of electric trucks queuing at charging stations
	c_w	Unit waiting time penalty for late arrival of trucks at the start depots of delivery tasks
	g	Charging rate of charging piles, i.e., the electricity charged per unit time
	h	Electricity consumption rate of electric trucks, i.e., the electricity consumed per unit time
	E	Battery capacity of electric trucks
	M	A sufficiently large positive number
	$n_{\max}$	Number of candidate charging stations
	$R_{n,\max}$	Maximum number of charging piles that can be installed at charging station n
	$V_{\max}$	Maximum number of electric trucks allowed to procured
	$C_{\max}$	Maximum number of charging stations allowed to be constructed in the area
	$Q_{\max}$	Total number of charging piles allowed to be installed across all charging stations
Variables	x_{ij}^v	Binary variable, $x_{ij}^v = 1$ if electric truck $v \in V$ goes directly from node $i \in N$ to node $j \in N$; otherwise, $x_{ij}^v = 0$
	Z_n	Binary variable, $Z_n = 1$ if a charging station is built at candidate location $n \in U$; otherwise, $Z_n = 0$
	r_j	Binary variable, $r_j = 1$ if a charging pile is installed at candidate charging pile node $j \in C$; otherwise, $r_j = 0$
	α_{ij}^{uv}	Binary variable, $\alpha_{ij}^{uv} = 1$ if electric truck $u \in V$ arrives at charging station $n \in U(\forall i, j \in C_n)$ earlier than electric truck $v \in V$; otherwise, $\alpha_{ij}^{uv} = 0$
	β_i^{uv}	Binary variable, $\beta_i^{uv} = 1$ if electric truck $u \in V$ arrives at charging pile $i \in C$ earlier than electric truck$v \in V$; otherwise, $\beta_i^{uv} = 0$
	θ^v	Binary variable, $\theta^v = 1$ if electric truck $v \in V$ is assigned delivery tasks; otherwise, $\theta^v = 0$
	τ_i^v	The time when electric truck $v \in V$ arrives at node $i \in N$
	s_i^v	The time when electric truck $v \in V$ starts charging at charging pile $i \in C$
	y_i^v	The SoC of electric truck $v \in V$ upon arrival at node $i \in N$
	η_i^v	The time when electric truck $v \in V$ departs from the customer node with start depot $i \in P$

3.1. Objective Function

The objective function (1) minimizes the total system cost for completing all delivery tasks. The first term represents the truck travel time costs on the road network; the second term captures delay penalties; the third term accounts for electricity consumption costs; the fourth term calculates the waiting time costs at charging stations; the fifth term covers truck procurement and maintenance costs; the sixth term captures the construction and maintenance costs of charging stations; and the final term represents the construction and maintenance costs of charging piles.

$$\begin{aligned}\min\ & c_t \sum_{v\in V}\sum_{i\in N}\sum_{j\in N} t_{ij}x_{ij}^{v} + c_w \sum_{v\in V}\sum_{i\in P}\left(n_i^v - a_i\right) \\ & + c_e \sum_{v\in V}\sum_{i\in C}\left(E - y_i^v\right) + c_q \sum_{v\in V}\sum_{i\in C}\left(S_i^v - \tau_i^v\right) \\ & + c_f \sum_{v\in V}\sum_{j\in P}\sum_{i\in O} x_{ij}^{v} + c_s \sum_{n\in U} Z_n + c_r \sum_{j\in C} r_j\end{aligned} \tag{1}$$

3.2. Constraints

The model is subject to constraints on (i) vehicle routing feasibility, (ii) operational timing (including service/travel times), (iii) charging principle, (iv) battery energy/SoC dynamics, and (v) budget availability.

3.2.1. Travel Route Constraints

Constraints (2)–(14) ensure that each electric truck follows the delivery workflow depicted in Figure 1. Truck v departs from its origin O, and picks up customer goods at node P, and then delivers them to the corresponding drop-off node D. If the SoC is insufficient to complete the next assigned task, the truck detours to a charging pile C and recharges to full power before resuming service. After completing all assigned delivery tasks, truck v returns to its designated return node T.

$$\sum_{v\in V} x_{i,i+\delta}^{v} = 1, \quad \forall i \in P \tag{2}$$

$$\sum_{v\in V}\sum_{j\in P\cup C\cup T\setminus\{i-\delta\}} x_{ij}^{v} = 1, \quad \forall i \in D \tag{3}$$

$$\sum_{v\in V}\sum_{j\in N} x_{ij}^{v} = 1, \quad \forall i \in P\cup D \tag{4}$$

$$\sum_{v\in V}\sum_{j\in O\cup D\cup C} x_{ij}^{v} = 0, \quad \forall i \in C \tag{5}$$

$$\sum_{v\in V}\sum_{j\in O\cup D\cup C\cup T} x_{ij}^{v} = 0, \quad \forall i \in O \tag{6}$$

$$\sum_{j\in P}\sum_{i\in O} x_{ij}^{v} \le 1, \quad \forall v \in V \tag{7}$$

$$\sum_{v\in V}\sum_{j\in N} x_{ij}^{v} = 0, \quad \forall i \in T \tag{8}$$

$$\sum_{j\in N} x_{ij}^{v} = \sum_{j\in N} x_{ji}^{v}, \quad \forall i \in D\cup P\cup C, \forall v \in V \tag{9}$$

$$\sum_{j\in N} x_{ij}^{v} - \sum_{j\in N} x_{j,i+\sigma+2\delta+Q_{\max}}^{v} = 0, \forall i \in O, \forall v \in V \tag{10}$$

$$\sum_{i\in P} x_{i,i+\delta}^{v} \ge 1 - M(1-\theta^v), \quad \forall v \in V \tag{11}$$

$$\sum_{i\in P} x_{i,i+\delta}^{v} \le M\theta^v, \quad \forall v \in V \tag{12}$$

$$1 - M(1-\theta^v) \le \sum_{j\in P}\sum_{i\in O} x_{ij}^{v} \le 1 + M(1-\theta^v), \forall v \in V \tag{13}$$

$$-M\theta^v \le \sum_{j\in P}\sum_{i\in O} x_{ij}^{v} \le M\theta^v, \quad \forall v \in V \tag{14}$$

Constraints (2)–(4) enforce a one-to-one correspondence between the start depot and the end depot for each delivery task. Specifically, from a pickup node $i \in P$, a truck may proceed only to its paired drop-off node $i + \delta \in D$. From a drop-off node $i \in D$, a truck

may proceed only to another unserved pickup node, a charging station or its final return node. By restricting each pickup node to be visited by one single truck, constraints (2)–(4) prevent multiple vehicles from executing the same delivery task.

Constraint (5) ensures that, after fully recharging at charging pile $i \in C$, a truck may only travel to a pickup node or to its return node. Constraint (6) restricts trucks departing from origin nodes $i \in O$ to proceed only to pickup nodes, while constraint (7) further ensures that, from any origin $i \in O$, at most one delivery task is assigned to each truck. Constraint (8) enforces work termination: once a truck reaches its return node T, it performs no further delivery tasks. Constraint (9) imposes flow balance at pickup nodes, drop-off nodes, and charging stations. Constraint (10) ensures that any truck departing from origin $i \in O$ will ultimately return to its designated terminal $i + \sigma + 2\delta + Q_{\max} \in T$.

It is worth noting that constraints (2)–(10) may lead to cyclic loops (subtours) as illustrated in Figure 3, whereby a truck circulates among pickup node P, drop-off node D, and charging station C without properly linking to an origin or return node. Accordingly, constraints (11)–(14) are added to eliminate such loops by enforcing that every feasible delivery route must start from an origin O and ultimately terminate at a return node T. Operationally, constraints (11)–(14) stipulate that if a truck executes any delivery task, i.e., transports customer goods from some pickup node i to its paired drop-off node $i + \delta$, then the truck must be deployed $(\theta^v = 1)$ and must depart from some origin in O. Conversely, if a truck performs no delivery task, it is inactive and does not need to be procured $(\theta^v = 0)$.

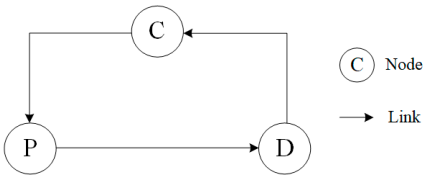

Figure 3. Schematic diagram of cyclic loop.

3.2.2. Operation Time Constraints

To reflect real-world logistic operations, the movement of electric trucks must satisfy a set of temporal constraints, which are shown below.

$$\tau_i^y = 0,\ \forall i \in O, \forall v \in V \tag{15}$$

$$\tau_i^v + t_{ij}x_{ij}^v - M(1 - x_{ij}^v) \le \tau_j^v,\ \forall i \in O \cup D, \forall j \in N, \forall v \in V \tag{16}$$

$$\tau_i^v + t_{ij}x_{ij}^v + M(1 - x_{ij}^v) \ge \tau_j^v,\ \forall i \in O \cup D, \forall j \in N, \forall v \in V \tag{17}$$

$$a_i \le \eta_i^v, \forall\ i \in P, \forall v \in V \tag{18}$$

$$\tau_i^v \le \eta_i^v, \forall\ i \in P, \forall v \in V \tag{19}$$

$$\eta_i^v + t_{ij}x_{ij}^v - M(1 - x_{ij}^v) \le \tau_j^v, \forall i \in P, \forall j \in N, \forall v \in V \tag{20}$$

$$\eta_i^v + t_{ij}x_{ij}^v + M(1 - x_{ij}^v) \ge \tau_j^v, \forall i \in P, \forall j \in N, \forall v \in V \tag{21}$$

$$\tau_i^v \le s_i^v, \forall\ i \in C, \forall v \in V \tag{22}$$

$$s_i^v + (E - y_i^v)/g + t_{ij}x_{ij}^v - M(1 - x_{ij}^v) \le \tau_j^v,\ \forall i \in C, \forall j \in N, \forall v \in V \tag{23}$$

$$s_i^v + (E - y_i^v)/g + t_{ij}x_{ij}^v + M(1 - x_{ij}^v) \ge \tau_j^v, \forall i \in C,\ \forall j \in N, \forall v \in V \tag{24}$$

Constraint (15) initializes the departure times of all the trucks from their origins. Constraints (16) and (17) ensure that when a truck leaves its origin node or a drop-off node, its arrival time at the next node j, τ_j^v, equals its arrival time at node i, τ_i^v, plus the travel time from i to j, t_{ij}. Constraint (18) ensures that a truck cannot depart from a pickup node

$i \in P$ before the start time of the delivery task a_i. Constraint (19) enforces causality at pickup nodes by requiring truck departure time η_i^v to be no earlier than its own arrival time τ_i^v. Constraints (20) and (21) ensure that when a truck leaves a pickup node, its arrival time at the next node τ_j^v equals its departure time η_i^v plus the travel time t_{ij}, i.e., $\tau_j^v = \eta_i^v + t_{ij}$. Constraint (22) stipulates that charging of a truck can only start after its arrival. Constraints (23) and (24) set post-charging timings by stating that the arrival time at the next node τ_j^v equals the charging start time s_i^v plus the required charging duration to full power $(E - y_i^v)/g$ and the travel time t_{ij} in between.

3.2.3. Charging Principle Constraints

It is assumed that electric trucks are served under a first-come-first-served principle upon arrival at charging stations. Accordingly, constraints (25)–(32) are introduced.

$$\tau_i^v \geq \tau_i^u - M(1 - \beta_i^{uv}), \forall v, u \in V, v \neq u, \forall i \in C \tag{25}$$

$$\tau_i^v \leq \tau_i^u + M\beta_i^{uv}, \forall v, u \in V, v \neq u, \forall i \in C \tag{26}$$

$$s_i^v \geq s_i^u + (E - y_i^u)/g - M(1 - \beta_i^{uv}), \forall v, u \in V, v \neq u, \forall i \in C \tag{27}$$

$$s_i^v + (E - y_i^v)/g \leq s_i^u + M\beta_i^{uv}, \forall v, u \in V, v \neq u, \forall i \in C \tag{28}$$

$$\tau_i^v \geq \tau_j^u - M\left(1 - \alpha_{ij}^{uv}\right), \forall v, u \in V, v \neq u, \forall i, j \in C_n, \forall n \in U \tag{29}$$

$$\tau_i^v \leq \tau_j^u + M\alpha_{ij}^{uv}, \forall v, u \in V, v \neq u, \forall i, j \in C_n, \forall n \in U \tag{30}$$

$$s_i^v \geq s_j^u - M\left(1 - \alpha_{ij}^{uv}\right), \forall v, u \in V, v \neq u, \forall i, j \in C_n, \forall n \in U \tag{31}$$

$$s_i^v \leq s_j^u + M\alpha_{ij}^{uv}, \forall v, u \in V, v \neq u, \forall i, j \in C_n, \forall n \in U \tag{32}$$

Constraints (25)–(28) encode the first-come-first-served principle at the pile level: if truck u arrives at charging pile $i \in C$ before truck v (i.e., $\beta_i^{uv} = 1$), then the charging start time of truck v at i must be no earlier than the charging end time of truck u. Otherwise, if $\beta_i^{uv} = 0$, then the charging start time of truck u at charging pile i must be no earlier than the charging end time of truck v.

Under constraints (25)–(28), pile-level schedules may still produce station-level anomalies contrary to basic queueing intuition. Figure 4 shows such an example, with a truck that arrived later joining a shorter queue so as to start charging earlier. To preclude such cases, constraints (29)–(32) are further constructed to enforce station-level first-come-first-served consistency. If truck u arrives at charging station $n \in U$ before truck v (i.e., $\alpha_{ij}^{uv} = 1$), then truck u will start charging at station n earlier than truck v. Otherwise, if $\alpha_{ij}^{uv} = 0$, then truck u will start charging later than truck v.

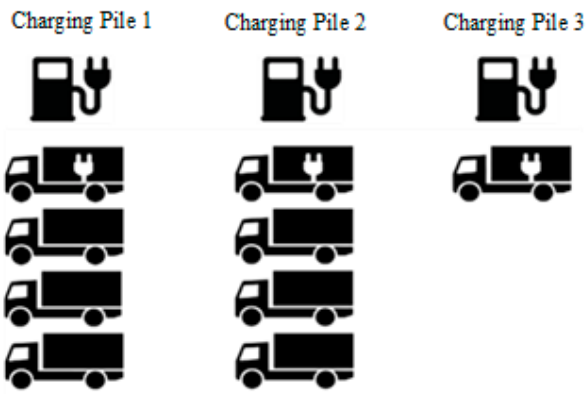

Figure 4. An example of an unrealistic charging queuing scenario.

3.2.4. Battery Dynamics Constraints

Electric trucks continuously consume battery energy during delivery service, and when necessary, they will detour to find charging stations. Constraints (33)–(37) describe such battery energy dynamics.

$$0 \le y_j^v \le y_j^v - hd_{ij}x_{ij}^v + E\left(1 - x_{ij}^v\right), \forall i \in P \cup D \cup O, \forall j \in N, \forall v \in V \tag{33}$$

$$y_j^v \ge y_j^v - hd_{ij}x_{ij}^v - E\left(1 - x_{ij}^v\right), \forall i \in P \cup D \cup O, \forall j \in N, \forall v \in V \tag{34}$$

$$y_j^v \le E - hd_{ij}x_{ij}^v, \quad \forall i \in C, \forall j \in N, \forall v \in V \tag{35}$$

$$r_j \ge x_{ij}^v, \quad \forall i \in D, \forall j \in C, \forall v \in V \tag{36}$$

$$y_i^v = E, \quad \forall i \in O, \forall v \in V \tag{37}$$

Constraints (33) and (34) calculate the battery level for each electric truck that departs from an origin node, pickup node or drop-off node. The battery level upon arrival at the next node j equals its battery level at the start node i minus the energy consumed to travel from i to j.

Constraint (35) specifies the target battery level of each vehicle once charged. Since the objective function (1) minimizes the charging cost, constraint (35) together with the objective function ensures that, for any truck departing from a charging pile i, its battery level upon arrival at the next node j satisfies $y_j^v = E - e_{ij}$, where E is the full battery level and e_{ij} is the energy consumed to reach j.

Constraint (36) means charging is only feasible at those nodes that at least one charging pile is installed. Finally, constraint (37) assumes all electric trucks start service at full charge.

3.2.5. Budget Constraints

Without loss of generality, budget constraints are imposed in terms of the total number and the capacities of the charging stations, as specified in constraints (38)–(41).

$$Z_n \ge r_j, \qquad \forall n \in U, \forall j \in C_n \tag{38}$$

$$\sum_{n \in U} Z_n \le C_{\max}, \qquad \forall n \in U \tag{39}$$

$$\sum_{j \in C_n} r_j \le R_{n,\max}, \qquad \forall j \in C_n, \forall n \in U \tag{40}$$

$$\sum_{j \in C} r_j \le Q_{\max}, \qquad \forall j \in C \tag{41}$$

Constraint (38) means a charging station is built at candidate location $n \in U$ only when it is necessary to install charging piles at this location. Constraint (39) caps the total number of stations to be built. Constraint (40) limits the number of charging piles installed at each station and constraint (41) bounds the network-wide number of charging piles allowed to be installed.

3.3. Model Summary

The explicit model derived is composed of the objective function (1) and the constraints (2)–(41). Both the objective function and all the constraints are linear, thus the formulation is a mixed-integer linear program. The integer decision variables include x_{ij}^v, Z_n, r_j, α_{ij}^{uv}, β_i^{uv}, and θ^v. The problem of siting and sizing of charging stations is NP-hard. The size of the model primarily grows with the number of binary variables contained. The time complexity to solve such a model is $O(2^n)$, where n is the number of binary variables.

4. Constraint Validation Tests

A series of validation tests are first conducted on a corridor network with seven nodes, as depicted in Figure 5. There are four delivery tasks, as detailed in Table 2. The optimization models derived can be directly solved with the dual simplex solver in the Gurobi 11.0.3 optimization platform (Gurobi Optimization, Beaverton, OR, USA). The results reported below are generated with a computer configured with an Intel(R) Core(TM) i5-7400 @ 3.00 GHz quad-core processor, 8 GB RAM and a 64-bit Windows 11 Professional operating system. Set the solver tolerance to 0.01%. The models in the five cases reported below are solved within several seconds.

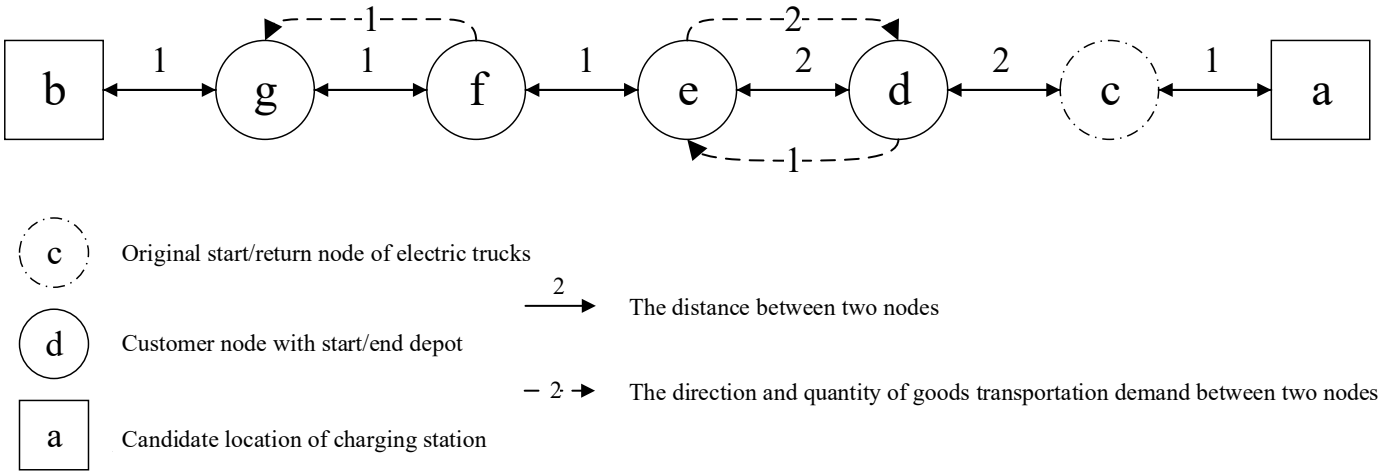

Figure 5. A corridor network with seven nodes.

Table 2. Details of the four delivery tasks in the corridor network.

Number	Pickup Node	Drop-Off Node	Start Time
1	f	g	4
2	e	d	15
3	e	d	18
4	d	e	23

The parameters used in this section are set for illustrative purposes. In practical applications, they need to calibrated based on real operational data. Here, trucks travel 1 unit distance per unit time; $c_t = 1$ is the unit travel time cost; $c_e = 0.5$ is the unit electricity cost; $c_q = 2$ is the unit waiting time cost at charging stations; $c_f = 50$ is the procurement and maintenance cost per electric truck; $c_s = 25$ is the construction and maintenance cost per charging station; $c_r = 5$ is the construction and maintenance cost per charging pile; at most $V_{\max} = 4$ trucks can be deployed; only $C_{\max} = 1$ charging station is to be built; the charging station allows installing only $R_{n,\max} = 1$ charging piles; the charging rate g and the energy consumption rate h are both set to be 10, and $E = 200$ is the battery capacity.

Case 1

With the unit late arrival penalty $c_w = 2$ at goods pickup nodes, the optimal objective value derived is 516.0. The charging station is built at node b. The travel routes of the four trucks are shown below.

$$v_1 : c \to e \to d \to b \to c$$

$$v_2 : c \to f \to g \to b \to c$$

$$v_3 : c \to d \to e \to b \to c$$

$$v_4 : c \rightarrow e \rightarrow d \rightarrow b \rightarrow c$$

The detailed travel and charging dynamics are provided in Table 3. The four trucks sequentially visit charging station b to be charged, in order of v_2, v_4, v_3, v_1. Since there is only one charging pile, a truck can only start charging after those previous trucks have arrived, thus queuing time will be incurred. v_2 is the first to get charged, with no waiting time at station b; v_4 arrives when v_2 has finished charging; v_3 and v_1 arrive at the same time, but neither can get charged upon arrival. They both wait in the queue until v_4 finishes charging at time 33, then v_3 starts charging first. v_3 finishes charging at time 40 when v_1 starts charging. Thus, v_3 and v_1 experience queuing times of 5 and 12, respectively.

Table 3. The travel dynamics and charging dynamics of electric trucks in Case 1.

Node i	**e**	**d**	**b**	**c**
$\tau_i^{v_1}$	4.0	23.0	28.0	58.0
$s_i^{v_1}$	-	-	40.0	-
$\eta_i^{v_1}$	21.0	-	-	-
$y_i^{v_1}$	160.0	140.0	90.0	190.0
Node i	**f**	**g**	**b**	**c**
$\tau_i^{v_2}$	5.0	6.0	7.0	21.0
$s_i^{v_2}$	-	-	7.0	-
$\eta_i^{v_2}$	5.0	-	-	-
$y_i^{v_2}$	150.0	140.0	130.0	190.0
Node i	**d**	**e**	**b**	**c**
$\tau_i^{v_3}$	2.0	25.0	28.0	47.0
$s_i^{v_3}$	-	-	33.0	-
$\eta_i^{v_3}$	23.0	-	-	-
$y_i^{v_3}$	180.0	160.0	130.0	190.0
Node i	**e**	**d**	**b**	**c**
$\tau_i^{v_4}$	4.0	17.0	22.0	40.0
$s_i^{v_4}$	-	-	22.0	-
$\eta_i^{v_4}$	15.0	-	-	-
$y_i^{v_4}$	160.0	140.0	90.0	190.0

Case 2

In this case, the unit late arrival penalty is changed to $c_w = 10$, while other settings are the same as in case 1.

The optimal objective value increases to 532.0. The charging station is again built at node b. The detailed travel and charging dynamics are provided in Table 4. The charging order changes to v_2, v_4, v_1, v_3. The high waiting penalty results in no additional dwelling times at goods pickup nodes. In this case, v_1 arrives at station b earlier than v_3. v_1 experiences a waiting time of 8 and gets charged at time 33. v_3 experiences a waiting time of 16 before v_1 finishes charging at time 44.

Table 4. The travel dynamics and charging dynamics of electric trucks in Case 2.

i	**e**	**d**	**b**	**c**
$\tau_i^{v_1}$	4.0	20.0	25.0	51.0
$s_i^{v_1}$	-	-	33.0	-
$\eta_i^{v_1}$	18.0	-	-	-
$y_i^{v_1}$	160.0	140.0	90.0	190.0

Table 4. *Cont.*

i	f	g	b	c
$\tau_i^{v_2}$	5.0	6.0	7.0	21.0
$s_i^{v_2}$	-	-	7.0	-
$\eta_i^{v_2}$	5.0	-	-	-
$y_i^{v_2}$	150.0	140.0	130.0	190.0
i	d	e	b	c
$\tau_i^{v_3}$	2.0	25.0	28.0	58.0
$s_i^{v_3}$	-	-	44.0	-
$\eta_i^{v_3}$	23.0	-	-	-
$y_i^{v_3}$	180.0	160.0	130.0	190.0
i	e	d	b	c
$\tau_i^{v_4}$	4.0	17.0	22.0	40.0
$s_i^{v_4}$	-	-	22.0	-
$\eta_i^{v_4}$	15.0	-	-	-
$y_i^{v_4}$	160.0	140.0	90.0	190.0

Cases 3–5

Here, the allowed number of charging stations increases to $C_{\max} = 2$ and the allowed number of charging piles to be instilled increases to $R_{n,\max} = 4$. In case 3, the construction and maintenance cost per charging pile $c_r = 5$. In cases 4 and 5, the costs per charging pile increase to $c_r = 15$ and $c_r = 40$. For the three cases, other settings remain the same as in Case 1. The charging dynamics of electric trucks at the charging stations for cases 3–5 are provided in Table 5.

Table 5. The charging dynamics of electric trucks in Cases 3–5.

Case 3 $c_r = 5$	Charging Station	a		b	
	Charging Pile	1	2	3	
	Electric Truck	v_4	v_2	v_1	v_3
	τ_i^v	23	20	28	7
	s_i^v	23	20	28	7
	y_i^v	110	110	130	130
Case 4 $c_r = 15$	Charging Station	a		b	
	Charging Pile	1		2	
	Electric Truck	v_1	v_4	v_2	v_3
	τ_i^v	20	23	7	28
	s_i^v	20	29	7	28
	y_i^v	110	110	130	130
Case 5 $c_r = 40$	Charging Station	b			
	Charging Pile	1			
	Electric Truck	v_1	v_2	v_3	v_4
	τ_i^v	22	28	28	7
	s_i^v	22	33	40	7
	y_i^v	90	130	90	130

In case 3, two charging stations are to be constructed, deploying a total of three charging piles. Station a is equipped with two piles, while station b is equipped with one.

Trucks v_2 and v_4 visit charging station a to be charged at two different charging piles, and trucks v_1 and v_3 visit charging station b to be charged at the same charging pile. All the vehicles are charged upon arrival at the charging stations, i.e., there is no charging waiting time.

In case 4, the cost per charging pile increases to 15. The optimal results show that two charging stations are to be constructed, each with one charging pile. Compared to case 3, the total number of charging piles reduces by one. Trucks v_1 and v_4 visit charging station a to be charged, and trucks v_2 and v_3 visit charging station b to be charged. Truck v_4 experiences a waiting time of 6 before truck v_1 finishes charging.

In case 5, the cost per charging pile further increases to 40. Only charging station b is built, with only one charging pile. All the vehicles are charged at station b using the same charging pile, incurring more charging waiting times. Truck v_2 experiences a waiting time of 5, and truck v_3 experience a waiting time of 12.

As depicted in Figure 6, when the unit cost of installing charging piles increases, the total number of piles installed gradually decreases, leading to increases in the charging waiting times of the electric trucks.

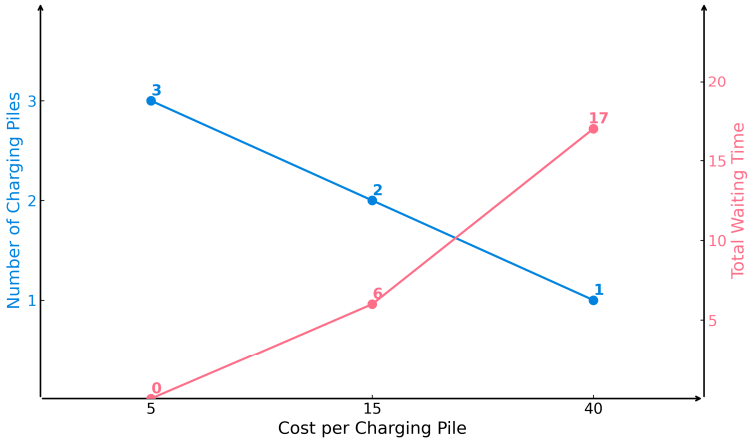

Figure 6. Results summary for cases 3–5.

5. Numerical Test on Falls Network

To validate the effectiveness of the proposed MILP model, a numerical test is further conducted on the Sioux Falls network. The network topology is shown in Figure 7, with 24 nodes and 76 links. The numbers on the links denote their lengths. Nodes 1, 2, 3, 4, 5, 7, 10, 11, 12, 13, 17, and 20 are the twelve optional original/return points for electric trucks, and nodes 5, 11, 15, 16, 20, and 23 are the six candidate locations of charging stations. There are 36 delivery tasks, as listed in Table 6, including, for each task, the pickup node, the drop-off node, and the task start time.

The other model parameters are set as follows: trucks travel 1 unit distance per unit time; $C_t = 1$ is the unit travel time cost; $C_e = 0.5$ is the unit electricity cost; $C_q = 2$ is the unit waiting time cost at charging stations; $C_w = 2$ is the unit late arrival penalty; $C_f = 50$ is the procure and maintenance cost per electric truck; at most $V_{\max} = 8$ trucks can be deployed; $C_s = 25$ is the construction and maintenance cost per charging station; at most $C_{\max} = 4$ charging stations can be built; $C_r = 5$ is the construction and maintenance cost per charging pile; each charging station allows installing at most $R_{n,\max} = 3$ charging piles; the system can install at most $Q_{\max} = 6$ charging piles in total; $g = 2$ is the charging rate; $h = 2$ is the energy consumption rate; and $E = 150$ is the battery capacity.

In this case, the optimization model is of manageable scale and can be solved directly with available commercial solvers. The dual simplex solver in the Gurobi 11.0.3 optimiza-

tion platform is employed again here. Set the solver tolerance to 0.01% and the computation time is around two and a half hours.

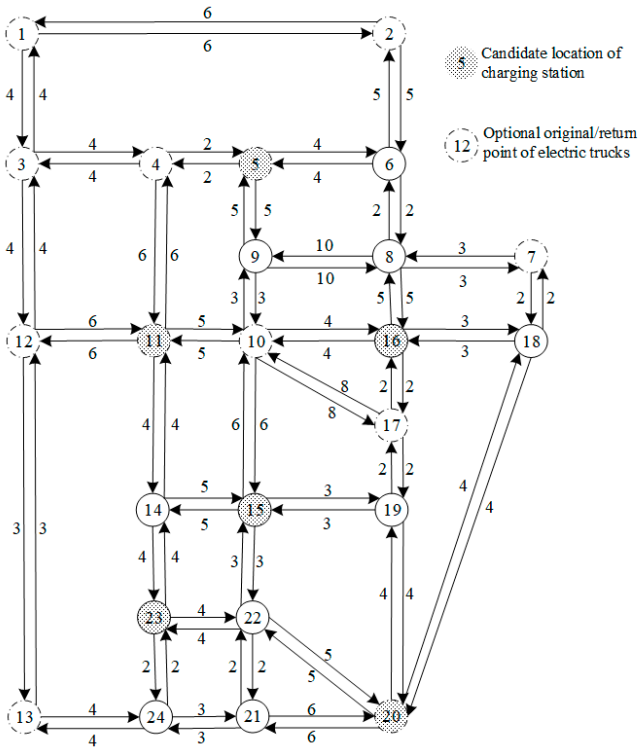

Figure 7. Topology of the Sioux Falls network.

Table 6. Details of the 36 delivery tasks in the Sioux Falls network.

Number	Pickup Node	Drop-Off Node	Start Time	Number	Pickup Node	Drop-Off Node	Travel Time
1	13	6	132	19	16	18	23
2	20	11	149	20	10	9	112
3	20	6	46	21	23	24	85
4	10	7	4	22	18	23	137
5	10	4	9	23	5	22	35
6	23	19	93	24	14	17	26
7	3	17	91	25	12	24	125
8	7	19	13	26	5	23	169
9	21	13	93	27	3	19	97
10	3	20	44	28	5	13	121
11	16	5	7	29	19	2	134
12	11	14	19	30	17	9	139
13	20	15	160	31	6	19	107
14	1	10	152	32	2	10	158
15	21	18	128	33	15	23	164
16	12	13	133	34	23	7	157
17	8	17	40	35	16	21	8
18	17	23	66	36	2	1	88

The optimal objective value or the minimum total system cost is 3869. The optimal locations of charging stations and the original/return nodes of electric trucks are shown in Figure 8. To complete all delivery tasks, five electric trucks are deployed and they depart from and return to four nodes: 7, 10, 11, and 17. Three charging stations are to be constructed to provide charging service to the trucks, located at nodes 11, 15, and 20.

Station 11 is equipped with two charging piles, Station 15 with one pile, and Station 20 with two piles.

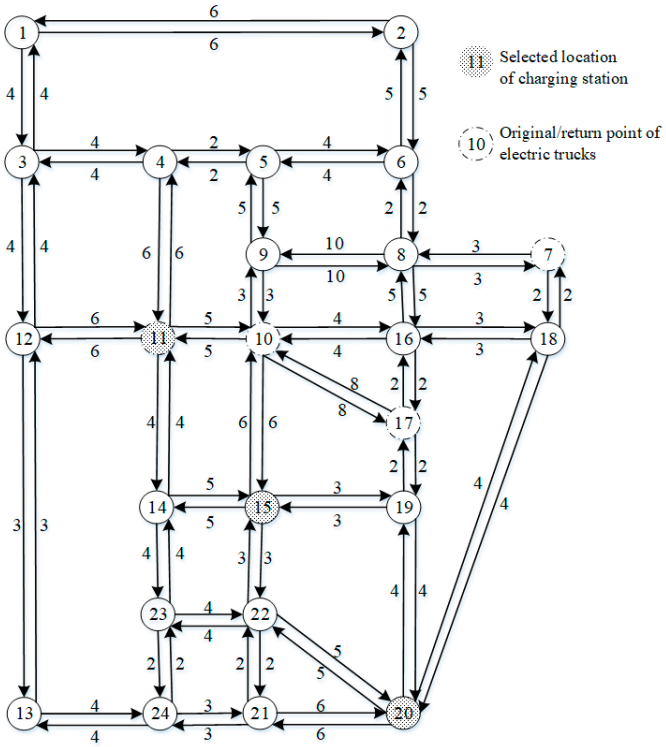

Figure 8. Optimal locations of charging stations and the original/return points of electric trucks in the Sioux Falls network.

Figure 9 further shows the detailed travel routes of the five electric trucks deployed. The numbers above the arrows correspond to the delivery task IDs in Table 2. Numbers in boxes (e.g., "$\boxed{20}$") indicate that the node hosts a charging station. Numbers with overlines (e.g., "$\overline{11}$") indicate that trucks arrive earlier than the start times of the deliver tasks; numbers with underlines (e.g., "$\underline{23}$") indicate that trucks arrive late. Vehicle 1 finishes eight delivery tasks and charges once at charging station 20. Vehicle 2 finishes nine delivery tasks and charges three times at charging stations 11 and 20. Vehicle 3 finishes six delivery tasks and charges twice at charging stations 15 and 20. Vehicle 4 finishes six delivery tasks and charges once at charging station 11. Vehicle 5 finishes seven delivery tasks and charges twice at charging stations 11 and 20. And all the trucks return to their original nodes after completing all the delivery tasks.

$$v_1: 11 \to \overline{11} \xrightarrow{12} 14 \to \overline{14} \xrightarrow{24} 17 \to 16 \xrightarrow{19} 18 \to \boxed{20} \to \underline{20} \xrightarrow{3} 6 \to \overline{2} \xrightarrow{36} 1 \to \overline{12} \xrightarrow{25} 24 \to \underline{23} \xrightarrow{6} 19 \to 17 \xrightarrow{30} 9 \to 11$$

$$v_2: 10 \to \overline{10} \xrightarrow{4} 7 \to \overline{7} \xrightarrow{8} 19 \to \boxed{20} \to \underline{8} \xrightarrow{17} 17 \to \overline{17} \xrightarrow{18} 23 \to \overline{23} \xrightarrow{21} 24 \to \overline{21} \xrightarrow{15} 18 \to \boxed{20} \to \underline{5} \xrightarrow{28} 13 \to \underline{13} \xrightarrow{1} 6 \to \boxed{11} \to \underline{3} \xrightarrow{7} 17 \to 10$$

$$v_3: 17 \to \overline{16} \xrightarrow{35} 21 \to 5 \xrightarrow{23} 22 \to \boxed{15} \to \underline{21} \xrightarrow{9} 13 \to \overline{12} \xrightarrow{16} 13 \to \underline{3} \xrightarrow{10} 20 \to \boxed{20} \to \underline{2} \xrightarrow{32} 10 \to 17$$

$$v_4: 7 \to \overline{6} \xrightarrow{31} 19 \to \overline{19} \xrightarrow{29} 2 \to 1 \xrightarrow{14} 10 \to \underline{10} \xrightarrow{20} 9 \to \boxed{11} \to \underline{18} \xrightarrow{22} 23 \to \underline{23} \xrightarrow{34} 7 \to 7$$

$$v_5: 17 \to \overline{16} \xrightarrow{11} 5 \to \underline{10} \xrightarrow{5} 4 \to \boxed{11} \to \overline{3} \xrightarrow{27} 19 \to \boxed{20} \to \overline{20} \xrightarrow{13} 15 \to 15 \xrightarrow{33} 23 \to \underline{20} \xrightarrow{2} 11 \to \underline{5} \xrightarrow{26} 23 \to 17$$

Figure 9. Delivery routes of electric trucks in the Sioux Falls network.

Table 7 summarizes the utilization of each charging station. The five trucks totally charge nine times at the three stations in order to complete all the delivery tasks. Three trucks (2, 4, and 5) visit station 11 and charge once each. Only truck 3 charges once at station 15. Four trucks (1, 2, 3, and 5) visit station 20, among which truck 2 charges twice there.

Table 7. Charging summary in the case of the Sioux Falls network.

Station Node	Charged Vehicles	Numbers of Charging
11	2 4 5	1 1 1
15	3	1
20	1 2 3 5	1 2 1 1

6. Hybrid Heuristic for Large Scale Networks

When applied to logistic problems in large scale networks, the proposed MILP will become intractable for commercial solvers, like the dual simplex solver in the Gurobi 11.0.3, due to combinatorial surges in integer variables. Accordingly, this section delivers a hybrid heuristic framework that integrates a rolling horizon scheme with a genetic algorithm. The algorithm features time window-based decomposition and dynamic fitness evaluation. The overall framework is shown in Figure 10.

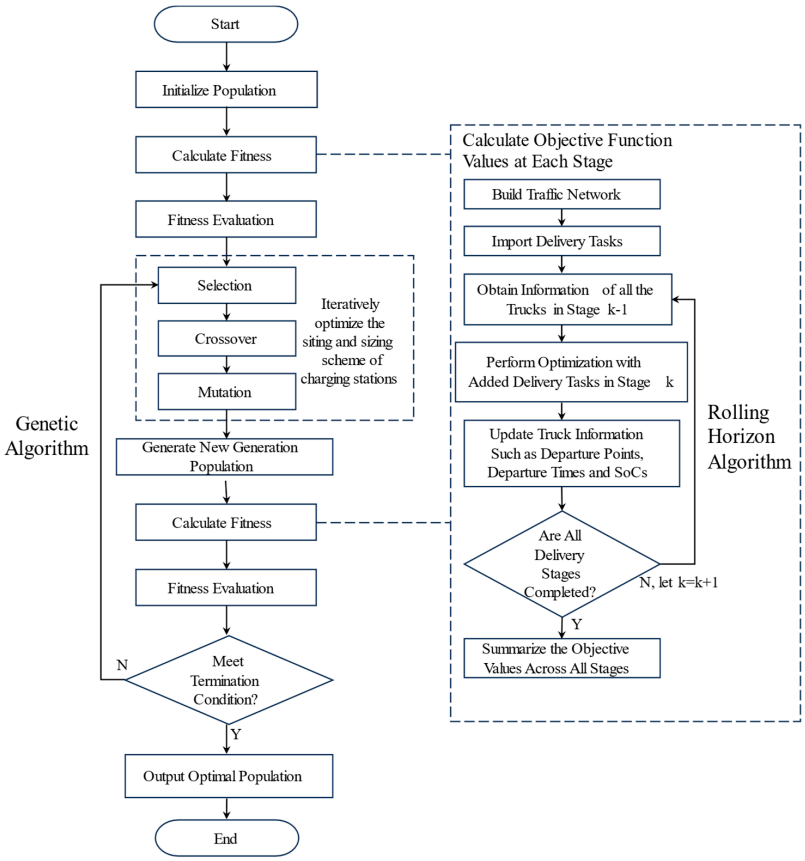

Figure 10. Solution algorithm framework for large-scale problems.

The rolling horizon mechanism essentially partitions the overall operating horizon into a sequence of time periods of equal length. Routing and charging decisions optimized in a previous period are rolled forward into the next period. The state of trucks at the end of a previous period, like their locations and SoCs, are regarded as the initial information for the next period. Such a mechanism is realized with the help of two node sets for virtual original nodes and virtual return nodes of electric trucks, as shown in Figure 11. At the end of a previous period, the virtual return nodes are utilized to help record all the truck information, like their locations, arrival times and SoCs. In the next period, all these virtual return nodes are turned into virtual origin nodes, and all the truck information will be fed into the next optimization subroutine. The pseudocode of the hybrid heuristic is provided in Algorithm 1 Pseudo-code of the hybrid heuristic.

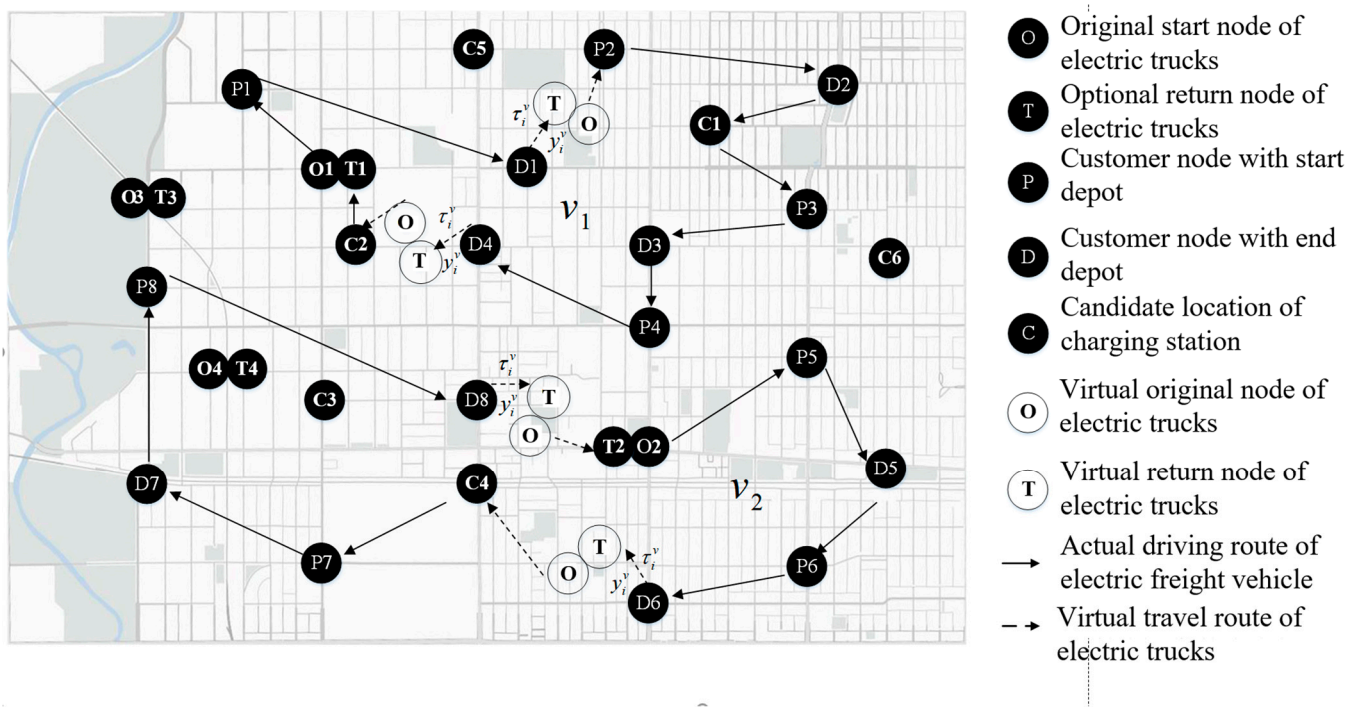

Figure 11. Virtual original nodes and virtual return nodes in rolling horizon algorithm.

Algorithm 1. A Siting and Sizing Algorithm for Charging Facilities in Large-Scale Road Networks

Step 1: Initialization

Step 1.1: Import Basic Data

Import the road network data, delivery order data, electric truck (ET) departure/return points, candidate sites for charging stations, and the shortest paths for all node pairs.

Step 1.2: Time Window Division

Divide the m-hour modeling horizon into s periods, each with a duration of t seconds. Allocate the delivery orders into these s periods based on the order start times.

Step 1.3: Parameter Setting Initialize parameters including travel speed, c_t, c_e, c_f, c_p, c_w, c_q, c_s, c_r, g, h and E.

Step 1.4: Population Initialization

Set the number of generations to be 0, i.e., gen = 0. Generate an initial population containing 10 individuals, i.e., the population size is 10.

Implement binary encoding, where 0 represents no charging station/pile is to be built at the node, and 1 represents one charging station/pile is to be built at the node.

Step 1.5: Truck Fleet Initialization

Initialize the states of all the electric trucks.

Algorithm 1. *Cont.*

Step 2: Fitness Evaluation
For each individual siting and sizing scheme in the population:
    Set the total system cost for completing all delivery tasks be zero, i.e., cost = 0
    For each time period k:
        Step 2.1: Construct Transport Network
        Import the delivery tasks for period k. Updated vehicle origin set *v_origin*. Construct the node sets O, P, D, C, T, N for the transport network and update the shortest paths for all node pairs.
        Step 2.2: Execute Period-k Optimization
        Solve the proposed MILP for time period k, to obtain the optimal vehicle routing plans, fleet size, and charging schemes for all the trucks in service, as well as the objective value k_cost. Update cost = cost + k_cost.
        Step 2.3: Acquire Period-k Vehicle Information
        Retrieve information for trucks operating in period k, including the vehicles in service, their start points, end points, SoCs, arrival times, and the charging piles used.
        Step 2.4: Update Truck Departure Points
        Send the locations of trucks at the end of period k to set *v_origin* as their start points in the next period k + 1. Update the set O.
    End For
    Record the fitness value, i.e., the total system cost, for each individual siting and sizing scheme.
    Update the best fitness value fit_{best} for each generation.
End For
Step 3 Population Update with Genetic Algorithm
    Update gen = gen + 1.
    If gen > gen_{max} = 50, terminate; otherwise:
        Keep the best two individuals in the last population.
        Step 3.1: Crossover
        Select two individuals from the last population. The selection probability is proportional to the fitness value.
        Perform uniform crossover on the two selected individuals to generate offspring. A crossover probability of 90% is applied.
        Repeat crossover until enough valid offspring are generated.
        Step 3.2: Mutation
        Perform scramble mutation on individuals after crossover. A mutation rate of 10% is applied.
        Repeat crossover until enough valid offspring are generated.
    Return to Step 2.
(Algorithm End)

7. Numerical Test on Chicago Network

Numerical test is further conducted on the Chicago network on a much larger-scale, as shown in Figure 12, which comprises 933 nodes and 2967 links (the detailed network data is available from the GitHub website). Assuming a total of 300 delivery tasks, we selected 20 nodes as optional origin/return points for electric trucks and 10 nodes as candidate locations for charging stations, as depicted in Figure 12. To save space, the detailed coordinates of these selected nodes are provided in Tables 8 and 9.

The other model parameters are set as follows: trucks travel 5 unit distance per unit time; $C_t = 1$ is the unit travel time cost; $C_e = 1$ is the unit electricity cost; $C_q = 2$ is the unit waiting time cost at charging stations; $C_w = 2$ is the unit late arrival penalty; $C_f = 100$ is the procurement and maintenance cost per electric truck; at most $V_{\max} = 20$ trucks can be deployed; $C_s = 80$ is the construction and maintenance cost per charging station; at most

$C_{\max} = 8$ charging stations can be built; $C_r = 10$ is the construction and maintenance cost per charging pile; each charging station allows installing up to $R_{n,\max} = 3$ charging piles; the system can install at most $Q_{\max} = 30$ charging piles in total; $g = 10$ is the charging rate; $h = 10$ is the energy consumption rate; and $E = 500$ is the battery capacity.

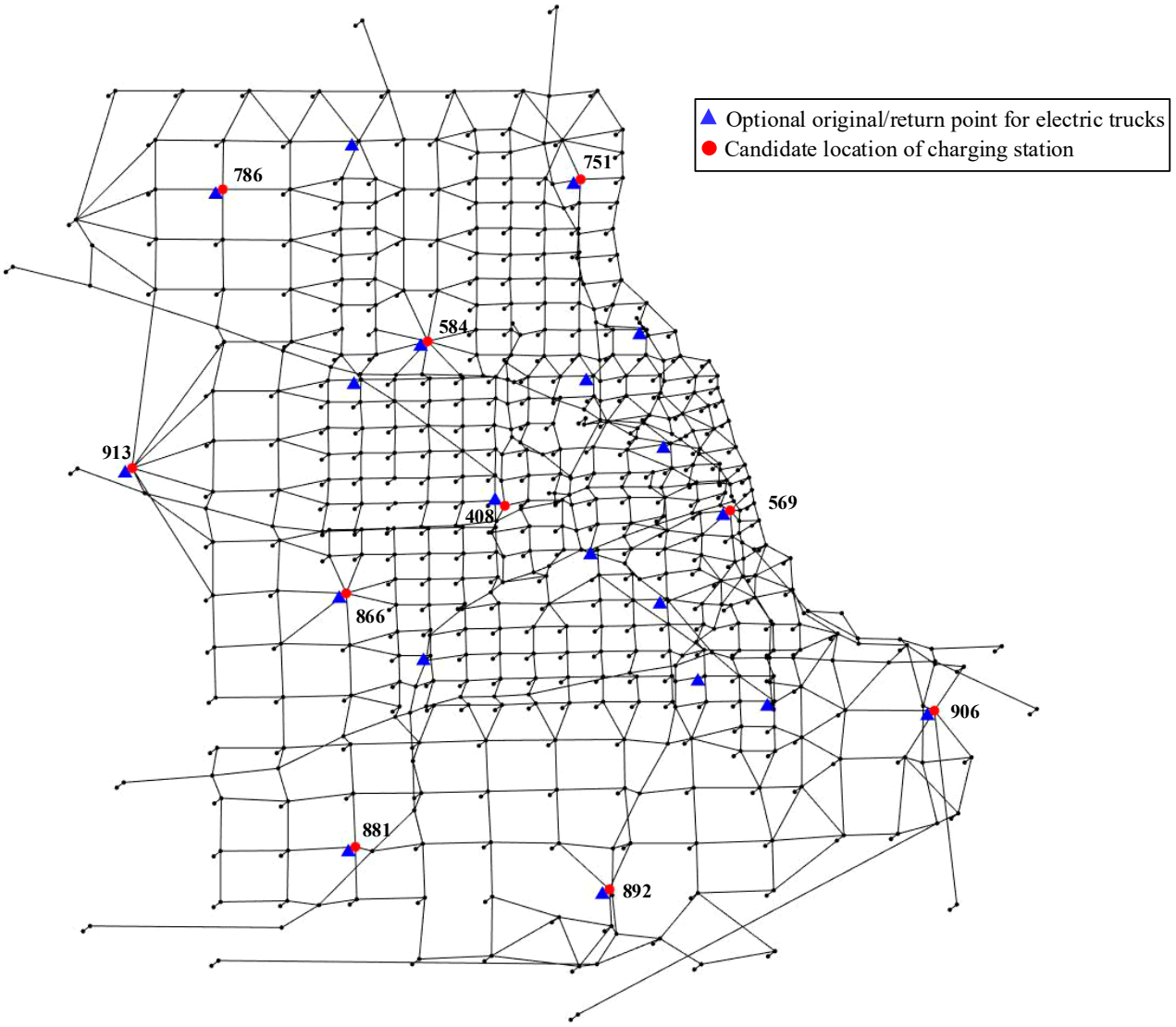

Figure 12. Chicago network topology and candidate locations of charging stations.

Table 8. The coordinates of the original/return nodes of electric trucks in the Chicago network.

Number	X-Coordinate	Y-Coordinate	Number	X-Coordinate	Y-Coordinate
367	10.37	63.623	47	55.083	79.727
240	18.239	96.0749	100	56.852	48.373
237	30.073	101.6869	10	57.157	66.49
170	30.256	73.932	346	51.85	14.579
38	36.051	78.3849	89	50.813	54.107
320	28.975	49.044	116	60.146	39.406
335	29.768	19.52	122	66.185	36.478
273	36.295	41.785	360	80.0929	35.38
689	42.517	60.451	23	62.342	58.682
67	50.447	74.3589	205	49.349	97.2339

Table 9. The coordinates of the candidate locations of charging stations in the Chicago network.

Number	X-Coordinate	Y-Coordinate
408	43.371	59.841
569	62.952	59.292
892	52.46	15.189
906	80.7029	35.99
866	29.585	49.654
881	30.378	20.13
751	49.959	97.8439
786	18.849	96.6849
584	36.661	78.9949
913	10.98	64.233

Given the scale of the Chicago network, the resulting optimization model cannot be directly solved by commercial solvers. The hybrid heuristic developed in Section 5 is applied here. The operation horizon is divided into time periods of 60 time units and the 300 delivery tasks are folded into corresponding time periods according to their start times. Utilizing the DEAP evolutionary algorithm toolbox [23] via the Python 3.11.5 API (Python Software Foundation, Beaverton, OR, USA), we build the genetic algorithm framework, and the dual simplex solver in Gurobi 11.0.3 is still applied for fitness evaluation.

The population size is set to be 10 per generation, and the crossover and mutation rates are 90% and 10%, respectively. Under these settings, it takes over 8 days to finish 50 iterations. The convergence curve of the algorithm is shown in Figure 13. It can be observed that the hybrid heuristic converges quickly, and, by the 9th generation, the fitness value has reached the minimum of 127,389.

The optimal siting and sizing scheme for charging stations is encoded as {[1, 1, 1],[1, 0, 1], [0, 0, 0], [0, 0, 0], [0, 0, 0], [0, 0, 0], [1, 0, 1], [1, 0, 1], [0, 0, 0]}; that is, a total of four charging stations are to be constructed at nodes 596, 892, 786, and 584, as depicted with charging symbols in Figure 12. Nice charging piles in total are to be installed in these four stations. The station located at node 569 installs three charging piles, and the stations at nodes 892, 786, and 584 each install two charging piles.

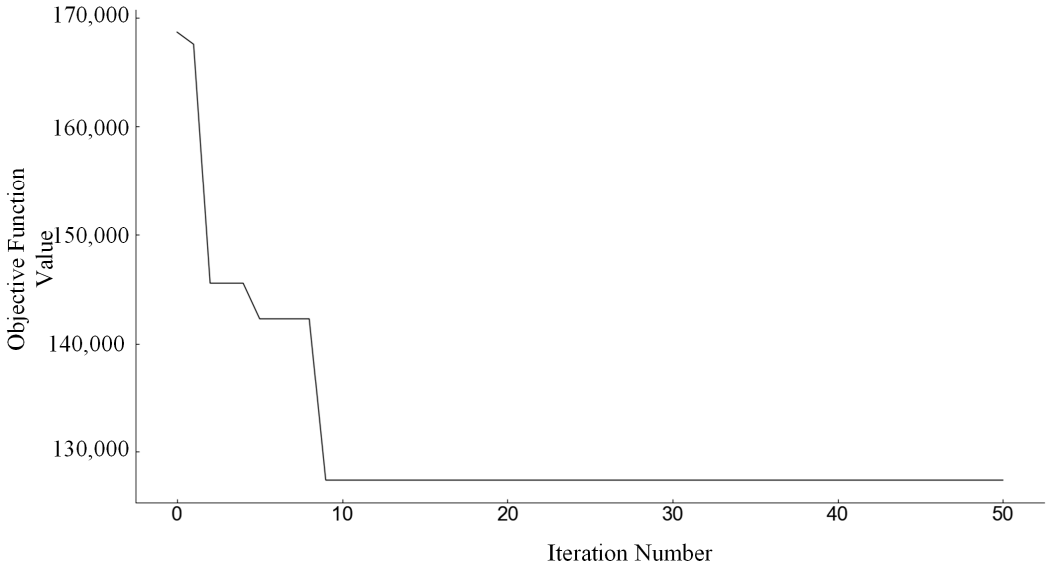

Figure 13. Convergence curve of the solution process for the Chicago network.

8. Conclusions

This paper addresses the problem of siting and sizing charging stations for electric freight trucks by developing an explicit mixed-integer linear program. The model enables the joint optimization of the siting and sizing of charging stations, as well as fleet size, routing, and charging decisions for electric trucks. The model incorporates queuing at charging stations by constructing a set of constraints that enforce the first-come-first-served principle, thereby explicitly quantifying the waiting times of the trucks across all the charging stations. For large-scale road networks with complex logistics scenarios, a hybrid heuristic algorithm is proposed that combines a rolling horizon framework with a genetic algorithm: the rolling horizon mechanism decomposes the original large-scale problems, and the global search capability of the genetic algorithm improves solution efficiency. Numerical experiments on a corridor network, the Sioux Falls network and the Chicago network demonstrate excellent optimization performance.

Future work may proceed in multiple directions. First, alternative solution approaches may be explored to improve solution efficiency for large scale problems. Second, based on the derived model, we plan to develop an adaptive charging strategy that dynamically adjusts the required charging amount for each truck based on its real-time task requirements and remaining SoC, so as to reduce charging times and queuing times at charging stations. Third, alternative queuing disciplines beyond the current first-come-first-served principle will be explored, which may provide more flexible and scenario-adaptive charging service rules for different logistics operation contexts. Finally, the siting and sizing of charging stations under stochastic demand may be investigated, so as to adapt to more realistic logistics scenarios.

Author Contributions: Conceptualization, Y.X. and L.Z.; methodology, Y.X. and X.S.; software, Y.X. and X.S.; validation, X.S. and Y.W.; formal analysis, Y.X. and X.S.; investigation, Y.W.; resources, Y.W.; data curation, Y.X.; writing—original draft preparation, Y.X. and X.S.; writing—review and editing, L.Z.; visualization, Y.X. and X.S.; supervision, L.Z.; project administration, L.Z.; funding acquisition, L.Z. All authors have read and agreed to the published version of the manuscript.

Funding: This work was supported in part by the Key Research and Development Program of Zhejiang Province under Grants 2022C01129 and the Balance Architecture Research Center of Zhejiang University.

Institutional Review Board Statement: Not applicable.

Informed Consent Statement: Not applicable.

Data Availability Statement: The data presented in this study are available on request from the corresponding author.

Acknowledgments: The authors are grateful to the editor and the anonymous reviewers for their insightful comments and suggestions.

Conflicts of Interest: The authors declare no conflicts of interest.

References

1. Soulopoulos, N.; McKerracher, C.; Fisher, R.; Yang, M. *Zero-Emission Commercial Vehicles: The Time Is Now*; Bloomberg New Energy Finance: London, UK, 2024.
2. Dua, R.; Almutairi, S. A perspective on emerging policy and economics research priorities for enabling low-carbon trucking. *Energy Res. Soc. Sci.* **2025**, *124*, 104025. [CrossRef]
3. Al-Hanahi, B.; Ahmad, I.; Habibi, D.; Masoum, M.A.S. Charging infrastructure for commercial electric vehicles: Challenges and future works. *IEEE Access* **2021**, *9*, 121476–121492. [CrossRef]
4. Link, S.; Stephan, A.; Speth, D.; Plötz, P. Rapidly declining costs of truck batteries and fuel cells enable large-scale road freight electrification. *Nat. Energy* **2024**, *9*, 1032–1039. [CrossRef]

5. Song, Y. Optimization of Electric Vehicles' Charging Station Location. Master's Thesis, Southwest Jiaotong University, Chengdu, China, 2016.
6. Zhu, Z.-H.; Gao, Z.-Y.; Zheng, J.-F.; Du, H.-M. Charging station location problem of plug-in electric vehicles. *J. Transp. Geogr.* **2016**, *52*, 11–22. [CrossRef]
7. Seifeddine, B.; Layeb, S.B. Determining optimal deployment of electric vehicles charging stations: Case of Tunis City, Tunisia. *Case Stud. Transp. Policy* **2019**, *7*, 628–642. [CrossRef]
8. Shang, X.; Wang, M.-J.; Xu, L.-X.; Zhang, L.-H. Configuration optimization of electric vehicle charging facilities in urban areas. *J. Zhejiang Univ. (Eng. Sci.)* **2020**, *54*, 1210–1217.
9. Xiao, B.; Gao, F. Optimization method of electric vehicle charging stations' site selection and capacity determination considering charging piles with different capacities. *Electr. Power Autom. Equip.* **2022**, *42*, 157–166.
10. Zhu, S.Y.; Yang, B.; Zhu, X.L. Location and capacity of electric vehicle charging stations considering deviation path. *J. Shanghai Marit. Univ.* **2019**, *40*, 44–50.
11. Sun, S.Z. Study on the Layout Planning of Charging Facilities and Optimization of Distribution Route for Pure Electric Logistics Vehicles. Master's Thesis, Jilin University, Changchun, China, 2020.
12. Wang, Y.; Zhou, J.; Sun, Y.; Wang, X.; Zhe, J.; Wang, H. Electric vehicle charging station location-routing problem with time windows and resource sharing. *Sustainability* **2022**, *14*, 11681. [CrossRef]
13. Wu, T.; Li, Z.; Wang, G.; Zhang, X.; Qiu, J. Low-carbon charging facilities planning for electric vehicles based on a novel travel route choice model. *IEEE Trans. Intell. Transp. Syst.* **2023**, *24*, 5908–5922. [CrossRef]
14. Kınay Ö, B.; Gzara, F.; Alumur, S.A. Charging station location and sizing for electric vehicles under congestion. *Transp. Sci.* **2023**, *57*, 1433–1451. [CrossRef]
15. Yi, Z.; Bauer, P.H. Optimal stochastic eco-routing solutions for electric vehicles. *IEEE Trans. Intell. Transp. Syst.* **2018**, *19*, 3807–3817. [CrossRef]
16. Owais, M.; Alshehri, A. Pareto optimal path generation algorithm in stochastic transportation networks. *IEEE Access* **2020**, *8*, 58970–58981. [CrossRef]
17. Almutairi, A.; Owais, M. Reliable Vehicle Routing Problem Using Traffic Sensors Augmented Information. *Sensors* **2025**, *25*, 2262. [CrossRef] [PubMed]
18. Setak, M.; Karimpour, A. A mathematical model for the electric vehicle routing with time windows considering queuing system at charging stations and alternative paths. *J. Ind. Syst. Eng.* **2019**, *12*, 284–306.
19. Li, B.; Jha, S.S.; Lau, H.C. Route planning for a fleet of electric vehicles with waiting times at charging stations. In Proceedings of the European Conference on Evolutionary Computation in Combinatorial Optimization (Part of EvoStar), Trieste, Italy, 23–25 April 2025; Springer International Publishing: Cham, Switzerland, 2019; pp. 66–82.
20. Chen, R.; Qian, X.W.; Miao, L.X.; Ukkusuri, S.V. Optimal charging facility location and capacity for electric vehicles considering route choice and charging time equilibrium. *Comput. Oper. Res.* **2020**, *113*, 104776. [CrossRef]
21. Uslu, T.; Kaya, O. Location and capacity decisions for electric bus charging stations considering waiting times. *Transp. Res. Part D Transp. Environ.* **2021**, *90*, 102645. [CrossRef]
22. Schoenberg, S.; Buse, D.S.; Dressler, F. Siting and sizing charging infrastructure for electric vehicles with coordinated recharging. *IEEE Trans. Intell. Veh.* **2022**, *8*, 1425–1438. [CrossRef]
23. Fortin, F.; De Rainville, F.; Gardner, M.; Parizeau, M.; Gagne, C. DEAP: Evolutionary algorithms made easy. *J. Mach. Learn. Res.* **2022**, *31*, 2171–2175.

Disclaimer/Publisher's Note: The statements, opinions and data contained in all publications are solely those of the individual author(s) and contributor(s) and not of MDPI and/or the editor(s). MDPI and/or the editor(s) disclaim responsibility for any injury to people or property resulting from any ideas, methods, instructions or products referred to in the content.